EFFECT OF DIFFERENT OPERATING PARAMETERS ON MORPHOLOGY AND DIAMETER OF SUPERCRITICAL ANTISOLVENT POWDERS

Iolanda De Marco*, Ernesto Reverchon

Department of Industrial Engineering, University of Salerno
Via Ponte Don Melillo, 1, 84084, Fisciano (SA), Italy

*idemarco@unisa.it; fax: +39-89-964057

ABSTRACT

Supercritical antisolvent precipitation (SAS) has been applied on a model compound, Gadolinium acetate (GdAc), to analyze the effect of different operating conditions on morphology and diameter of precipitates.
The precipitation pressure has been varied from 90 to 200 bar, the precipitation temperature from 35 to 60 °C and the concentration of GdAc in dimethylsulfoxide (DMSO) from 20 to 300 mg/mL.
The results obtained can be explained in terms of competition between two characteristic times: the time of jet break-up and the dynamic surface tension vanishing time. The first one is related to droplets formation, the second one to gas mixing. We have shown that the cited process parameters can influence these times, and therefore the morphology of the resulting precipitates. In particular, when jet break–up prevails, sub–microparticles, or microparticles deriving from micro–droplets drying, are produced; when gas mixing is the governing process, nanoparticles are consistently produced by precipitation from the supercritical solution.

INTRODUCTION

The supercritical antisolvent process (SAS) has been successfully used to micronize different kinds of compounds [1-5]. Nanoparticles with mean diameters in the 30–200 nm range [6], spherical microparticles in the 0.25–20 μm range [7], expanded (hollow) microparticles with diameters between about 10 and 200 μm [8] have been extensively produced, varying the operating parameters.
Nevertheless several authors have studied the effect of the operating parameters on the particle size (PS) and particle size distribution (PSD) [9-14] of powders, only few attempts at analyzing the SAS precipitation mechanisms in terms of jet fluid dynamics, surface tension variation, mass transfer, vapor liquid equilibria (VLEs), nucleation and growth processes have been done [4,6-9,15-21].
In previous works, a correlation between particles dimensions and position of the SAS operating point in the vapor–liquid equilibria diagram has been proposed. At pressures far above the mixture critical point (MCP) pressure, nanoparticles can be precipitated [6,22]; near above the MCP, microparticles can be obtained [7]; whereas, operating at subcritical conditions, expanded microparticles [8] are produced.

The results obtained operating at different pressures have been related to the competition between the SAS characteristic phenomena that are the jet break-up of the liquid injected in the precipitator and the gas mixing. When jet break-up prevails, liquid droplets are formed and micrometric particles are produced; when gas mixing develops in the precipitator without jet break-up, droplets are not formed and nanoparticles precipitated from the fluid phase. Considering the competition between the characteristic times related to these two processes, it is possible to schematize: when the time for jet break-up (T) is shorter than time occurring for the vanishing of the dynamic surface tension (t), droplets are formed; in the opposite case, gas mixing prevails [4,7].
In this work, using a model compound previously processed by SAS [23], gadolinium acetate (GdAc), we attempt an analysis on the effect of temperature and concentration of the liquid solution, on the mechanisms of solute precipitation in terms of process characteristic times. The experiments performed varying the pressure confirmed the results obtained for other compounds and the experiments performed varying temperature and starting concentration of the liquid solution showed that the different characteristic particle diameters can be produced also operating at constant pressure. These information were assembled to obtain a more comprehensive scheme of the mechanisms controlling SAS precipitation.

MATERIALS AND METHODS

Gadolinium acetate (GdAc, purity 99.9%) and dimethyl sulfoxide (DMSO, purity 99.5%) were supplied by Sigma−Aldrich (Italy). CO_2 (purity 99%) was purchased from SON (Italy). All materials were used as received.
The SAS laboratory apparatus used in this work is schematically represented in **Figure 1**.

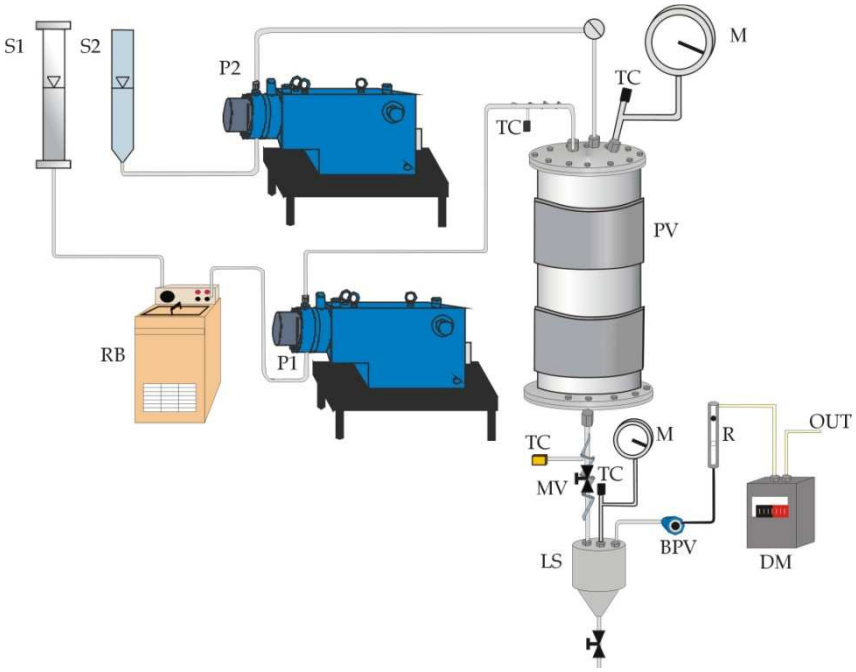

Figure 1: Schematic representation of a SAS apparatus. S1: CO_2 supply; S2: liquid solution; RB: refrigerating bath; P1, P2: pumps; TC: thermocouple; M: manometer; PV: precipitation vessel; MV: micrometering valve; LS: liquid separator; BPV: back pressure valve; R: rotameter; DM: dry test meter.

It consists of an HPLC pump (P2) used to deliver the liquid solution (S2), and a diaphragm high-pressure pump (P1) used to deliver carbon dioxide (S1). A cylindrical vessel with an internal volume of 500 cm^3 was used as the precipitation chamber (PV). The liquid mixture was delivered to the precipitator through a thin wall stainless steel nozzle with a 100 µm diameter.
A second collection chamber (LS) located downstream the precipitator at a lower pressure (18–20 bar) was used to recover the liquid solvent.
A SAS experiment begins delivering supercritical CO_2 at a constant flow rate to the precipitation chamber, until the desired pressure is reached. Then, pure solvent is sent through the nozzle in the precipitator to obtain steady state composition conditions of the fluid phase during the solute precipitation. When steady state conditions are established, the flow of the liquid solvent is stopped and the liquid solution is delivered through the nozzle at a given flow rate, producing the precipitation of the solute. At the end of the liquid solution delivery, supercritical CO_2 continues to flow to wash the chamber, eliminating the solution formed by the liquid solubilized in the supercritical antisolvent. If the final purge with pure CO_2 is not performed, the solvent contained in the fluid phase condenses during the depressurization step and can solubilize or modify the precipitates. At the end of the washing step, CO_2 flow is stopped and the precipitator is depressurized down to atmospheric pressure.
Samples of the precipitated powders were observed by a Field Emission Scanning Electron Microscope (FESEM), after coating with a conductive material.
Powders particle size distributions (PSDs) were measured from FESEM images using the Sigma Scan Pro image analysis software (release 5.0, Aspire Software International, USA); at least, five scanning electron microscope images, taken at high enlargements and in various locations inside the precipitator, were analysed in the elaboration of each distribution.

RESULTS AND DISCUSSION

The experiments were performed using DMSO as the liquid solvent, fixing the solution flow rate at 1 mL/min and adapting correspondingly SC-CO_2 flow rate to produce a $x_{CO2} \approx 0.97$.

Effect of pressure
First of all, the effect of pressure was studied to confirm results previously obtained with other compounds. Once fixed the temperature at 40 °C and the liquid solution concentration at 60 mg/mL, the pressure was varied between 90 and 200 bar.
At 90 bar, expanded microparticles were obtained, in the range 120–180 bar, microparticles were produced, whereas, at 200 bar, nanoparticles were obtained. These results confirmed the ones previously obtained [6-8,10,11,14], that, in some cases, were interpreted in terms of position of the operating point with respect to the MCP of the system DMSO–CO_2.
Considering the previous cited characteristic times, it is important to note that the jet break-up depends on pressure, therefore, increasing the pressure, the operating point moves from a subcritical phase to a near critical and then to a completely developed supercritical condition. At pressures lower than MCP pressure, the surface tension is always present, therefore EMP were obtained; at pressures higher that MCP pressure, the competition between the two times have to be considered. If $T<t$, microparticles formed from the droplets; if $T>t$ (at higher pressures), nanoparticles precipitated from a gas plume.

Effect of concentration

To perform this set of experiments, we fixed the pressure at 150 bar, the temperature at 40 °C, and we varied the concentration of the liquid solution from 20 to 300 mg/mL.

At 20 and 25 mg/mL, nanoparticles were obtained, in the range 30-120 mg/mL, microparticles were obtained, whereas between 160 and 300 mg/mL, expanded microparticles were obtained. Some examples of these morphologies are represented in **Figure 2**.

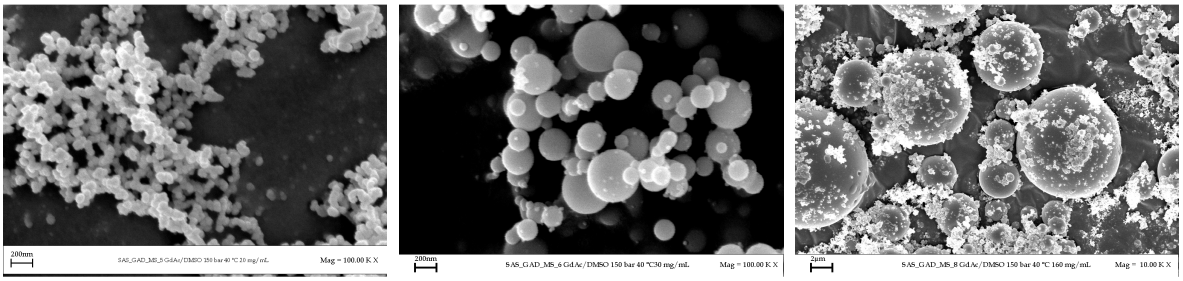

Figure 2: FESEM images of GdAc precipitated at 150 bar, 40 °C at different concentrations of the liquid solution; (a) nanoparticles obtained at 20 mg/mL; (b) microparticles obtained at 30 mg/mL; (c) expanded microparticles obtained at 160 mg/mL.

Also the effect of concentration can be explained in terms of characteristic times. Indeed, jet break-up depends not only on pressure, but also on the characteristic of the liquid jet, such as viscosity and surface tension. Increasing the concentration of the liquid solution, an increase of viscosity is obtained, therefore, the cohesive forces acting on the jet are higher (Re number decreases) and T increases. But, the presence of solute also modifies the evolution of the dynamic surface tension. Indeed, larger concentration gradients are formed during mixing between carbon dioxide and liquid solution, because a larger quantity of solute molecules are present; this causes an increase of the dynamic surface tension vanishing time; i.e., t increases. It means that, also in correspondence of completely developed supercritical conditions (at 150 bar, for example), when T<t, the morphology changes from nanoparticles to microparticles. At very high concentrations, the dynamic surface tension not reached the zero value at the end of microparticles precipitation and the particles continue to enlarge.

Effect of temperature

For this set of experiments, the pressure was fixed at 150 bar, the concentration of the liquid solution at 60 mg/mL and the process temperature was varied from 35 to 60 °C.

In the range 35-50 °C, microparticles were obtained, whereas, at 60 °C, expanded microparticles were precipitated. In this case, nanoparticles were not observed, probably due to the limited range of temperatures explored.

The temperature has an opposite effect with respect to pressure: the MCP of the liquid solution-supercritical antisolvent system, when temperature increases, moves to higher pressures, so the distance between the MCP and the operating point reduces.

Therefore, the mechanism of formation changes, since, at higher temperatures, the competition between T and t can give the results characteristic of near critical conditions (T < t). Therefore, the results related to pressure and temperature variations can be explained through the modification of the relative position of the SAS operating point and the MCP in the VLE diagram with temperature and on the consequent modifications of the characteristic times T and t. Summarizing, the experiments at increasing temperatures show a precipitation mechanism sequence that is the inverse of the one observed for pressure increasing.

CONCLUSIONS

The effect of the commonly considered SAS process parameters has been systematically studied; the formation of particles morphologies and diameters has been correlated with the competition between the time of jet break-up and the time of the surface tension vanishing, therefore the interpretation of SAS precipitation mechanisms in terms of characteristic times, previously done in dependence of the precipitation pressures can be extended.
A more comprehensive picture of the interactions among VLEs, fluid dynamics and mass transfer, during SAS precipitation is obtained and the competition of mechanisms previously proposed [4,7] is confirmed in this extended interpretation.
In our opinion, this is a general behavior observable for all the compounds that precipitate as amorphous particles [10,11], therefore these interpretations can be extended also to other compounds.
A final consideration is related to the transitions between one kind of particles to the other: it is a common tendency to consider sharp transitions; but, in the liquid jet, in principle it could be also possible that near the transition point (for example, from NP to MP) the length of the jet could be characterized by a jet break-up, immediately followed by SC mixture formation. In that case, nanoparticles and microparticles can coexist and could be collected together at the end of the experiment.

REFERENCES

[1] SHARIATI, A., PETERS, C. J., Current Opinion in Solid State & Materials Science, Vol. 7 (4–5), **2003**, p. 371.
[2] HAKUTA, Y., HAYASHI, H, ARAI, K., Current Opinion in Solid State & Materials Science, Vol. 7 (4–5), **2003**, p. 341.
[3] REVERCHON, E., J. Supercritical Fluids, Vol. 15 (1), **1999**, p. 1.
[4] REVERCHON, E., TORINO, E., DOWY, S., BRAEUER, A., LEIPERTZ, A., Chemical Engineering J., Vol. 156 (2), **2010**, p. 446.
[5] ELIZONDO, E., CÓRDOBA, A., SALA, S., VENTOSA, N., VECIANA, J., J. Supercritical Fluids, Vol. 53 (1–3), **2010**, p. 108.
[6] REVERCHON, E., DE MARCO, I., TORINO, E., J. Supercritical Fluids, Vol. 43 (1), **2007**, p. 126.
[7] REVERCHON, E., ADAMI, R., CAPUTO, G., DE MARCO, I., J. Supercritical Fluids, Vol. 47 (1), **2008**, p. 70.
[8] REVERCHON, E., DE MARCO, I., ADAMI, R., CAPUTO, G., J. Supercritical Fluids, Vol. 44 (1), **2008**, p. 98.
[9] SARKARI, M., DARRAT, I., KNUTSON, B. L., AIChE J., Vol. 46 (9), **2000**, p. 1850.
[10] REVERCHON, E., DE MARCO, I., DELLA PORTA, G., International J. Pharmaceutics, Vol. 243, **2002**, p. 83.
[11] REVERCHON, E., DE MARCO, I., J. Supercritical Fluids, Vol. 31 (2), **2004**, p. 207.
[12] TENORIO, A., GORDILLO, M. D., PEREYRA, C., MARTINEZ DE LA OSSA, E. J., J. Supercritical Fluids, Vol. 40 (2), **2007**, p. 308.
[13] KIM, M.-S., LEE, S., PARK, J.-S.,WOO, J.-S, HWANG, S.-J., Powder Technology, Vol. 177 (2), **2007**, p. 64.
[14] DE MARCO, I., REVERCHON, E., Powder Technology, Vol. 183 (2), **2008**, p. 239.

[15] LENGSFELD, C. S., DELPLANQUE, J. P., BAROCAS, V. H., RANDOLPH, T. W., J. Physical Chemistry B, Vol. 104, **2000**, p. 2725.
[16] BADENS, E., BOUTIN, O., CHARBIT, G., J. Supercritical Fluids, Vol. 36 (1), **2005**, p. 81.
[17] GOKHALE, A., KHUSID, B., DAVE, R. N., PFEFFER, R., J. Supercritical Fluids, Vol. 43 (2), **2007**, p. 341.
[18] OBRZUT, D. L., BELL, P. W., ROBERTS, C. B., DUKE, S. R., J. Supercritical Fluids, Vol. 42 (2), **2007**, p. 299.
[19] WERLING, J. O., DEBENEDETTI, P. G., J. Supercritical Fluids, Vol. 16 (2), **1999**, p. 167.
[20] WERLING, J. O., DEBENEDETTI, P. G., J. Supercritical Fluids, Vol. 18 (1), **2000**, p. 11.
[21] CHAVEZ, F., DEBENEDETTI, P. G., LUO, J. J., DAVE, R. N., PFEFFER, R., Industrial & Engineering Chemical Research, Vol. 42(13), **2003**, p. 3156.
[22] CHANG, S.–C., LEE, M.–J., LIN, H.–M., Chemical Engineering J., Vol. 139, **2008**, p. 416.
[23] REVERCHON, E., DE MARCO, I., DELLA PORTA, G., J. Supercritical Fluids, Vol. 23, **2002**, p. 81.